Published in final edited form as:

Cancer Res. 2018 June 01; 78(11): 2911–2924. doi:10.1158/0008-5472.CAN-17-1051.

Osteoblast-secreted factors mediate dormancy of metastatic prostate cancer in the bone via activation of the TGFβRIII-p38MAPK-pS249/T252RB pathway

Li-Yuan Yu-Lee[5], **Guoyu Yu**[1], **Yu-Chen Lee**[1], **Song-Chang Lin**[1], **Jing Pan**[5], **Tianhong Pan**[3], **Kai-Jie Yu**[1], **Bin Liu**[4], **Chad J. Creighton**[6], **Jaime Rodriguez-Canales**[1], **Pamela A. Villalobos**[1], **Ignacio I. Wistuba**[1], **Eulalia de Nadal**[7], **Francesc Posas**[7], **Gary E. Gallick**[2], and **Sue-Hwa Lin**[1,2]

[1]Department of Translational Molecular Pathology, The University of Texas M. D. Anderson Cancer Center, Houston, Texas 77030, USA

[2]Department of Genitourinary Medical Oncology, The University of Texas M. D. Anderson Cancer Center, Houston, Texas 77030, USA

[3]Department of Orthopedic Oncology, The University of Texas M. D. Anderson Cancer Center, Houston, Texas 77030, USA

[4]Center for Cancer Genetics and Genomics and Department of Genetics, The University of Texas M. D. Anderson Cancer Center, Houston, Texas 77030, USA

[5]Departments of Medicine and Molecular and Cellular Biology, Baylor College of Medicine, Houston, Texas 77030, USA

[6]Dan L. Duncan Cancer Center, Baylor College of Medicine, Houston, Texas 77030, USA

[7]Departament de Ciencies Experimentals i de la Salut, Universitat Pompeu Fabra, E-08003 Barcelona, Spain

Abstract

Bone metastasis from prostate cancer (PCa) can occur years after prostatectomy, due to reactivation of dormant disseminated tumor cells (DTC) in the bone, yet the mechanism by which DTC are initially induced into a dormant state in the bone remains to be elucidated. We show here that the bone microenvironment confers dormancy to C4-2B4 PCa cells, as they become dormant when injected into mouse femurs but not under the skin. Live-cell imaging of dormant cells at the single cell level revealed that conditioned medium from differentiated, but not undifferentiated osteoblasts induced C4-2B4 cellular quiescence, suggesting that differentiated osteoblasts present locally around the tumor cells in the bone conferred dormancy to PCa cells. Gene array analyses identified GDF10 and TGFβ2 among osteoblast-secreted proteins that induced quiescence of C4-2B4, C4-2b, and PC3-mm2, but not 22RV1 or BPH-1 cells, indicating PCa tumor cells differ

Correspondence: Sue-Hwa Lin, Department of Translational Molecular Pathology, Unit 89, The University of Texas M. D. Anderson Cancer Center, 1515 Holcombe Blvd., Houston, TX 77030. Phone: 713-794-1559; Fax: 713-834-6084; slin@mdanderson.org; or Li-Yuan Yu-Lee, Department of Medicine, Baylor College of Medicine, One Baylor Plaza, Houston, Texas 77030. Phone: 713-798-4770; Fax: 713-798-2050;: yulee@bcm.edu.

Conflict of interest: The authors declare no potential conflicts of interest.

in their dormancy response. TGFβ2 and GDF10 induced dormancy through TGFβRIII to activate phospho-p38MAPK, which phosphorylates RB at the novel N-terminal S249/T252 sites to block PCa cell proliferation. Consistently, expression of dominant-negative p38MAPK in C4-2b and C4-2B4 PCa cell lines abolished tumor cell dormancy both in vitro and in vivo. Lower TGFβRIII expression in PCa patients correlated with increased metastatic potential and decreased survival rates. Together, our results identify a dormancy mechanism by which DTC are induced into a dormant state through TGFβRIII-p38MAPK-pS249/pT252-RB signaling and offer a rationale for developing strategies to prevent PCa recurrence in the bone.

Keywords

dormancy; osteoblasts; GDF10; TGFβ2; prostate cancer

Introduction

Prostate cancer (PCa) can be effectively treated by surgery when the disease is localized. However, bone metastasis can occur decades after prostatectomy in some patients (1). Recurrence is likely due to reactivation of disseminated tumor cells (DTCs) that had been dormant at the metastatic site in bone. Because most therapies mainly target proliferating tumor cells, tumor dormancy is one mechanism for tumor cells to relapse at a later time. How DTCs initially become dormant in bone remains largely unknown.

Metastasis is attributed to interaction of tumor cells (seed) with the microenvironment of the metastasized organs (soil). Signaling in the bone microenvironment may regulate the switch between dormancy and proliferation of DTCs. Tumor dormancy may be mediated through different cell types present in the bone microenvironment. However, PCa preferentially metastasizes to bone and has unique interactions with osteoblasts (2). The differentiation state of osteoblasts in the bone microenvironment may influence the switch between dormancy versus proliferation in DTCs. At present, little is known about prostate tumor dormancy in bone as this disease state is not observed in clinical settings until the tumors have exited dormancy and progressed into overt bone metastasis. Understanding the mechanism(s) leading to dormancy of metastatic PCa in bone will provide a rationale for developing strategies to prevent PCa recurrence in bone.

In this study, we used intrabone and intracardiac injection models and established that the bone microenvironment can induce prostate tumor dormancy. We found that secreted factors from differentiated osteoblasts can induce cellular quiescence in some PCa cell lines but not in others, suggesting heterogeneity in dormancy response of prostate tumors. We further identified that osteoblast-secreted factors, including GDF10 and TGFβ2, induce tumor dormancy through activation of the TGFβRIII-p38MAPK-phospho(S249/T252)-RB signaling pathway and that inhibition of p38MAPK activation abrogates prostate tumor dormancy in bone.

Materials and Methods

Cell lines, antibodies and reagents

Cell lines: Human PCa C4-2B4 (gift from Robert Sikes, University of Delaware, 2006) (3,4), C4-2b (gift from Leland Chung, Cedars-Sinai Medical Center, 2004) (5), PC3-mm2 (gift from Isaiah J. Fidler, M.D. Anderson Cancer Center, 2005), 22Rv1 (ATCC, 2015) (6,7), and BPH-1 (gift from Simon Hayward, Vanderbilt University, 2015); mouse osteoblast precursor MC3T3 (ATCC, 2006); human lung carcinoma A549 (ATCC, 2013). The identity of all cell lines was verified by polymorphic Short Tandem Repeat loci (STR) profiling, and all cell lines are mycoplasma free. Recombinant human proteins: TGFβ2, TGFβ1, GDF10 (BMP-3b) (R&D). Antibodies: phospho-p38MAPK, p38MAPK, RB, Smad2/3, phospho-Smad1/5, p27Kip1, GAPDH, β-actin (Cell Signaling); phospho(S249/T252)-RB (8); Ki-67 (Dako); TGFβ2 and TGFβRIII (Proteintech); GDF10, p21 and TGFβRIII (R&D); β-tubulin, α-tubulin (GeneTex). Reagents: mouse TGFβ2 (Genorise) and osteocalcin (Alfa Aesar) ELISA kits; p38MAPK inhibitor SB202190 (InvivoGen); Vybrant DiO lipophilic membrane dye (Invitrogen).

Subcutaneous, intra-femural, and intracardiac injection of PCa cells

Luciferase-expressing PCa cells were injected under the skin, into the femurs (9), or into the left ventricle (10) of male SCID mice. Tumor growth was monitored using bioluminescence imaging. Animal studies were performed in accordance with as well as approved by an Institutional Animal Care and Use Committee (IACUC).

Immunohistochemistry

Tumor bearing femurs were fixed in formaldehyde and decalcified with formic acid before embedded in paraffin. Immunohistochemistry was performed as described (11).

Differentiation of primary mouse osteoblasts

Primary mouse osteoblasts (PMOs) were isolated from calvariae of 2-5 day-old pups, cultured to confluence, and the medium switched to differentiation medium, which contains ascorbic acid and β-glycerol phosphate. Osteoblast conditioned medium (OB-CM) was concentrated and medium exchanged by Centricon (Millipore) centrifugation.

Gene array analysis

RNAs prepared from undifferentiated and differentiated PMOs were subjected to whole-genome microarray analysis (4×44K, Agilent Technologies) (Arraystar, Inc). Array data are deposited in NCBI GEO under accession number GSE90127.

PCR

RNAs from PMOs were analyzed by qRT-PCR using mouse primers (Supplementary Table S1). Total DNA was prepared from mouse hind legs and used for real-time PCR using primers for human *Alu* repetitive sequences (Supplementary Table S1). The number of tumor cells in bone was calculated based on *Alu* PCR of a serial dilution of DNA from C4-2B4 cells.

Live-cell time-lapse imaging

PCa cells were plated in Hi-Q4 dishes (Ibidi) and cultured in RPMI-1650 containing 1:20 dilution of Day 0, 6, 24 or 30 OB-CM or in RPMI-1640 containing 0.1% FBS with TGFβ2, GDF10 or TGFβ1. Images were acquired every 20 min for 72 h in a BioStation (Nikon). Grid-500 glass-bottom dishes (Ibidi) were used for live-cell monitoring in more fields. Data were compiled using NIS-Elements (Nikon) software.

Immunofluorescence imaging

Following live-cell imaging, cells were fixed and permeabilized, co-incubated with anti-Ki67 and anti-p27, and re-imaged on the BioStation.

Proximity ligation assay (PLA)

Proximity ligation assay was performed using Duolink PLA In Situ Green Starter Kit (Mouse DUO92004/Rabbit DUO92004, Sigma). Primary antibodies were anti-phospho-p38MAPK (28B10) and anti-phospho-(S249/T252)-RB (8). Images were acquired using FluoView 1000 IX2 confocal microscopy (Olympus).

Generation of C4-2B4 cells with knockdown of TGFβRIII

TGFβRIII was knocked down by RNA interference via lentivirus-expressing shRNAs in pGIPZ. Clones C4-2B4-pGIPZ-sh-TβRIII #2 and #3 were generated. Antisense sequences for sh-TβRIII Clone #2: 5′-ATAGCTCCATGTTGAAGGT-3′ (NM_001195683) and Clone #3: 5′-ATAGTAGACCACACCATCA-3′ (MN_003243).

Generation of C4-2B4 and C4-2b cells with dominant-negative p38MAPK

C4-2B4 and C4-2b cells were transduced with retroviral-expressing p38α dominant-negative MAPK (p38DN), containing mutations in the activation loop between the two kinase domains, from Thr180-Gly-Tyr182 to Ala180-Gly-Phe182 (12), in a pBMN-I-GFP vector.

Human PCa datasets

The Kaplan-Meier method with log-rank test was used to evaluate overall disease-specific survival curves for PCa patients from the Nakagawa dataset (13). Patients from the Taylor data set (14) were used to evaluate PCa metastasis. Patients from the Lapointe dataset (15) were used to evaluate PCa metastatic progression. For computing *TGFBR3* gene score based on expression profiling data from human PCa tumors, *TGFBR3* gene was first *z*-normalized to SD from the median across the primary tumor samples. The average of the *z*-normalized values was used to represent the score for each sample profile.

Statistical analysis

Data quantification was performed by using the Student's *t*-test and expressed as mean ± s.e.m. *P* values of < 0.05 were considered statistically significant.

Results

C4-2B4 becomes dormant when injected into bone but not subcutaneous sites

The LNCaP subline C4-2B4 cells (3,4) labeled with luciferase and red fluorescence protein Tomato (C4-2B4-LT) (11) were injected subcutaneously or intrafemurally into SCID mice. While C4-2B4-LT grew exponentially under the skin, C4-2B4-LT grew slowly in mouse femurs, as quantified by bioluminescence over 5 weeks (Fig. 1A) and by histological analysis (Fig. 1B). We examined whether the limited tumor growth in bone might be due to increased cellular dormancy. Dormant cells have been characterized as non-proliferating, slow-cycling (16,17), and Ki-67 negative (18). C4-2B4-LT cells showed strong Ki-67 staining in subcutaneous tumors, but weak, diffuse staining in femoral tumors (Fig. 1B). Further, we examined the expression of G0/G1 markers, the p27 and p21 cell cycle inhibitors (19,20), in the tumors, and found p27 and p21 staining in C4-2B4 femoral tumors but little to no staining in subcutaneous tumors (Fig. 1C). These results suggest that the bone microenvironment provides factors that induce dormancy of C4-2B4 cells.

Conditioned media from differentiated mouse osteoblasts (OB-CM) lead to quiescence of C4-2B4 cells

We hypothesized that some dormancy-inducing factors in the bone microenvironment are secreted from osteoblasts. Primary mouse osteoblasts (PMOs) were cultured in differentiation media for 30 days. Osteoblast differentiation markers alkaline phosphatase and osteocalcin increased at 18 and 21 days, respectively (Fig. 1D) (21). Increases in dentin matrix protein (mDMP1) and sclerostin (mSOST-1), two osteocyte markers (21), were also detected at Day 24 and Day 30, respectively (Fig. 1D).

We prepared conditioned media from these differentiating osteoblasts (OB-CM) and examined C4-2B4 cellular response by live-cell imaging. When treated with non-differentiated Day 0 OB-CM for 72 h, the majority of C4-2B4 cells underwent several cell divisions with ~10% of cells non-proliferating or slow-cycling (Fig. 1E, 1F). When treated with Day 6, 24, or 30 OB-CM, ~20–35% of cells were non-proliferating (Fig. 1E, 1F), with little cell death (~1%) observed. Quiescent cells exhibited a low level of movement with cell shape changes observed during time-lapse (Fig. 1E, cells a–d). While proliferating cells were Ki-67 positive, OB-CM-treated non-proliferating C4-2B4 cells were Ki-67 negative (Fig. 1E, Day 0 versus Days 6–30). These observations suggest that factors in OB-CM from differentiated osteoblasts are capable of inducing cellular quiescence of C4-2B4 cells.

TGFβ2 and GDF10 are upregulated during osteoblast differentiation

To identify the dormancy factors from differentiated osteoblasts, we performed a gene array analysis using RNAs prepared from undifferentiated (Day 0) versus differentiated (Day 30) osteoblasts. The levels of 1844 and 1873 mRNAs were upregulated and downregulated with >2-fold change, respectively (see GSE90127). 194 genes encoding secretory proteins, including chemokines, cytokines and peptide growth factors, were upregulated in differentiated PMOs (Supplementary Table S2). Selected factors were further categorized into three groups based on p values (Fig. 2A and Supplementary Table S3). The p values were determined from duplicate samples used for the gene array analysis. Some of the

factors have high fold of differences but less consistent fold changes in duplicate samples and this has resulted in less significance in their p values. In group 1, increases in CXCL12, GDF10, TGFβ2, CCL4 and CCL12 levels were highly significant, with $p<0.001$ and false discovery rate (FDR) <0.15. Notably, the expression of TGFβ2, a factor shown to induce dormancy in various cancers (16–18,22), was increased 2.5-fold with $p=0.0008$ (FDR<0.14) in differentiated osteoblasts. GDF10 (BMP-3b) is a member of the TGFβ family and its role in dormancy is unknown.

We next confirmed the expression of TGFβ and GDF family proteins in Day 0 versus Day 27 osteoblasts. Among TGFβ family, expression of TGFβ1 and TGFβ2 was increased by 17- and 26-fold, respectively, at Day 27 of osteoblast differentiation (Fig. 2B). Among GDF family, GDF10 expression increased 8-fold, while GDF2 and GDF15 increased 2- 3-fold (Fig. 2B). Specifically, TGFβ2 mRNA levels increased ~20-fold over 30 days of osteoblast differentiation, but were undetectable in control undifferentiated osteoblast precursor MC3T3-E1 cells (Fig. 2C, upper). Immunoblot of the corresponding OB-CM confirmed an increase in secreted TGFβ2 during osteoblast differentiation (Fig. 2C, lower). GDF10 mRNA and protein also increased with similar kinetics as TGFβ2 (Fig. 2C). In contrast, TGFβ1 exhibited a different pattern of gene expression, increasing at Day 6 and remaining elevated to Day 30 (Fig. 2D). Thus, differentiated osteoblasts secrete factors such as TGFβ2 and GDF10 (Fig. 2E) that may play a role in inducing cellular quiescence of PCa cells.

TGFβ2 and GDF10 induce quiescence of C4-2B4 cells

Dormant cells are defined as “non-proliferating or slow-cycling cells, negative/low for proliferation markers and positive/high for CDK inhibitor expression” (16,23). Using these characteristics, we examined the potential dormancy-inducing activity of TGFβ2 and GDF10 on C4-2B4 cells using live-cell imaging over 72 h. TGFβ2 at 50 ng/ml (1 nM) and as low as 10 ng/ml (200 pM) significantly increased the level of quiescent C4-2B4 cells relative to untreated cells (Fig. 3A). TGFβ2-treated C4-2B4 cells that did not divide were negative for the proliferation marker Ki-67 (Fig. 3B, cells a–d) but stained positive for the CDK inhibitor p27 in the nucleus, suggesting that TGFβ2 induces cell cycle arrest leading to cellular dormancy.

A role of GDF10 in tumor dormancy has never been examined. GDF10 significantly increased the level of quiescent C4-2B4 cells (Fig. 3A). GDF10-treated quiescent cells were Ki-67 negative but showed strong p27 positivity in the nucleus (Fig. 3C, cells a–d), suggesting that GDF10 is a novel dormancy-inducing factor for C4-2B4 cells. TGFβ1 did not induce significant cellular quiescence in C4-2B4 cells (Fig. 3A), in agreement with reports that TGFβ1 does not affect dormancy in HNSCC HEp3 (16) and breast cancer cells (18).

TGFβ2 and GDF10 induce long-term dormancy in C4-2B4 cells

While most of the studies on cellular dormancy have been performed using a 48-h time frame (16,17,24), we next measured cellular dormancy over a much longer period, that is, over 7 days. C4-2B4 cells were labeled with the lipophilic membrane dye DiO (green), seeded in Grid-500 dishes to allow for cell monitoring in more fields, and followed for 7

days. The intensity of the photostable fluorescent DiO dye was diluted out by cell division in proliferating cells (Supplementary Fig. S1A) but not in non-proliferating cells (Supplementary Fig. S1B). We found that there was a higher number of DiO-positive cells with TGFβ2 (13.1% ± 2.3 %) or GDF10 (11.1 ± 3.0 %) treatment compared to untreated control cells (3.4% ± 0.8 %) over this extended period of time (Supplementary Fig. S2A). Further, these long-term DiO-positive cells also stained positive for p27 (Supplementary Fig. S2B, cells a and b). We followed some of the DiO-labeled quiescent PCa cells over 2 – 3 weeks (Supplementary Fig. S2C, S2D) and did not observe cell proliferation, suggesting that these cells represent long-term "slow-cycling or non-proliferating" dormant cells. These results suggest that TGFβ2 or GDF10 can induce long-term cellular dormancy in C4-2B4 cells. Moreover, removal of TGFβ2 or GDF10 from long-term dormant cells was unable to release cells from dormancy, suggesting that the simple removal of a factor may not be sufficient for dormant PCa cells to exit dormancy and resume cell proliferation. However, we cannot exclude the possibility that this is due to limitations of in vitro tissue culture conditions.

TGFβ2 and GDF10 induce quiescence in other PCa cells

We found that both TGFβ2 and GDF10 also increased cellular quiescence in C4-2b cells (5) and PC3-mm2 cells (25), but not 22Rv1 (7) and BPH-1 (26) cells (Fig. 3D). Although both C4-2b (5) and C4-2B4 (3,4) are LNCaP sublines, we found by live-cell imaging that they have slightly different cell morphology and properties under the same culture conditions. C4-2b cells tend to form aggregates and are more mobile in the culture dish, while C4-2B4 cells are more dispersed, flattened and less mobile (Supplementary Fig. S3A). These results show a differential response of PCa cell lines to dormancy induction by TGFβ2 and GDF10.

Knockdown of TGFβRIII in C4-2B4 cells prevents dormancy induction

TGFβ2 or GDF10 likely induces dormancy response through membrane receptors. TGFβ2 receptor is composed of TGFβRI, TGFβRII, and TGFβRIII (or betaglycan). TGFβRIII is particularly important as TGFβ2 cannot bind TGFβRII independently without TGFβRIII as a co-receptor (27). GDF10 receptor is reported to be TGFβR1 and TGFβRII in several cell lines (28–30). Whether TGFβRIII is required for GDF10 to function is unknown. We knocked down TGFβRIII, a proteoglycan with a 110-kDa core protein (31) that migrates as a diffuse band between 110-kDa to 200-kDa (Fig. 4A). Two clones, C4-2B4-shTβRIII-#2 and #3, both showing a ~60% decrease in TGFβRIII, lost dormancy response to TGFβ2 or GDF10, while sh-Vector control cells remained responsive (Fig. 4B), suggesting that TGFβRIII regulates both TGFβ2 and GDF10 signaling in dormancy induction in C4-2B4 cells.

TGFβ2 and GDF10 stimulate nuclear translocation of p-p38MAPK in PCa cells

Increases in cellular quiescence by TGFβ2 or GDF10 may be due to a switch from a mitogenic to a dormancy pathway, e.g., from ERK to p38MAPK (p38) signaling (32–34). While TGFβ family proteins activate the canonical Smad pathway (35,36), they also signal through non-canonical (p38MAPK, ERK1/2, PI3K/Akt) pathways (37,38). We found that p38MAPK was localized in the cytoplasm of C4-2B4 cells, but became enriched in the nucleus in response to TGFβ2 (Fig. 4C, left), indicating p38MAPK activation. p38MAPK

activation is accompanied by dual-phosphorylation of pThr180/pTyr182 (p-p38) (12) and p-p38 translocation into the nucleus. Both TGFβ2 and GDF10 stimulated p-p38 nuclear translocation within 30 min up to 3 h stimulation of C4-2B4 cells (Fig. 4C, right); this effect was strongly inhibited by the p38MAPK inhibitor SB202190 (Supplementary Fig. S3B). TGFβ2 and GDF10 also stimulated p-p38 nuclear translocation in C4-2b, PC3-mm2 (Fig. 4D) and C4-2B4-sh-Vector cells (Fig. 4E), but not C4-2B4-shTβRIII-#2 and #3 cells. In contrast, little activation of Smad signaling was observed (Supplementary Fig. S3C–S3F). These results suggest that activation of a TGFβRIII-p38MAPK signaling pathway mediates cellular quiescence in PCa cells.

N-terminal pS249/pT252 phosphorylation of RB by p38MAPK during dormancy induction in PCa cells

Nuclear p-p38 may increase cellular quiescence by modulating the activity of cell cycle regulatory proteins. p-p38 has recently been shown to phosphorylate the novel N-terminal Ser249/Thr252 sites in the tumor suppressor Retinoblastoma (RB) protein (8). p38-mediated phosphorylation of Ser249/Thr252-RB renders RB insensitive to cyclin-dependent kinase regulation, resulting in a delay in G1 cell cycle progression (8). Both TGFβ2 and GDF10 increased pS249/pT252-RB in the nucleus within 30 min of stimulation, a timing that closely followed p-p38 nuclear translocation (Fig. 5A). To detect potential physical association of endogenous pS249/pT252-RB with p-p38, we performed a proximity ligation assay (PLA) (39,40). We found a significant increase in PLA signals, visualized as individual fluorescent spots, in the nucleus of TGFβ2- or GDF10-treated cells relative to control cells (Fig. 5B, see enlarged), supporting an interaction between p-p38 and its substrate pS249/pT252-RB. As pS249/pT252-RB exhibits enhanced RB's repressor activity (8), these results suggest that p38MAPK-pS249/pT252-RB signaling blocks cell cycle progression, leading to cellular quiescence.

Expression of dominant-negative p38MAPK in PCa cells prevents dormancy induction in vitro

Next, we stably transduced C4-2B4 cells with p38α dominant-negative MAPK (p38DN) (12). Overexpression of p38DN did not affect the basal level of p-p38 expression (Fig. 6A). However, p38DN overexpression prevented nuclear translocation of p-p38 in C4-2B4-p38DN cells (Fig. 6B) and blocked dormancy induction in response to TGFβ2 and GDF10 (Fig. 6C). In contrast, robust nuclear translocation of p-p38 (Fig. 6B) and dormancy induction (Fig. 6C) was observed in C4-2B4-Vector control cells in response to TGFβ2 or GDF10. Similarly, overexpressing p38DN in C4-2b cells (Fig. 6D) blocked nuclear translocation of p-p38 (Fig. 6E) and prevented dormancy induction in C4-2b-p38DN cells (Fig. 6F) in response to either TGFβ2 or GDF10, while dormancy induction was not affected in C4-2b-Vector control cells. Thus, activation of p38MAPK signaling is required for TGFβ2- and GDF10-mediated dormancy induction in PCa cells.

Expression of dominant-negative p38MAPK in PCa cells abrogates dormancy in bone

We further injected C4-2B4-p38DN cells intrafemorally to examine their response to the dormancy-inducing activity in the bone microenvironment. C4-2B4-p38DN cells showed an increase in tumor growth in femur over 6 weeks, while C4-2B4-Vector control cells showed

an overall dormant phenotype (Fig. 7A). Close monitoring of individual mouse injected with C4-2B4-Vector cells showed fluctuations in tumor growth (Supplementary Fig. S4A), likely reflecting the failure of PCa micrometastases to expand in the dormancy-inducing microenvironment of the bone. Consistently, femoral tumors from C4-2B4-Vector cells revealed areas of cell death (Fig. 7Bi, asterisk), resulting in fewer viable cells, and weak and diffuse Ki-67 staining (Fig. 7Bii). In contrast, femoral tumors from C4-2B4-p38DN cells showed an abundance of mitotic figures (Fig. 7Biii, arrowheads; enlarged) and strong Ki-67 positivity (Fig. 7Biv). Quantification confirmed significant increases in the number of nuclei that have moderate to strong Ki-67 positivity in the C4-2B4-p38DN tumors compared to C4-2B4-Vector tumors (Fig. 7C). Similar growth kinetics (Supplementary Fig. S4B, S4C) and increases in moderate to strong Ki-67 positive nuclei were also observed in C4-2b-p38DN tumors compared to C4-2b-Vector tumors (Supplementary Fig. S4D).

Because disseminated tumor cells (DTCs) arrive in bone through the circulation, we also delivered tumor cells by intracardiac injection of PCa cells. We did not detect overt tumor growth in bone over 19 weeks by bioluminescence imaging. However, we detected human *Alu* repetitive sequence signals at the single cell level in total femur and tibia DNA prepared from mouse hind legs, as determined by real-time PCR using a serial dilution of DNA prepared from C4-2B4 cells (Fig. 7D). These results showed that C4-2B4 cells could disseminate to bone through intracardiac injection. At 1 week post-injection, the number of cells was around 350 ± 66 cells/leg (Fig. 7D, left panel), i.e., about 0.035% of the tumor cells per one million cells injected. These observations indicated that C4-2B4 cells have disseminated to bone and are consistent with clinical observations that few DTCs (<0.1%) survive to be detected in distant organs (41). At 5 weeks post-injection, the number of cells was about 7,699 ± 4,270 cells/leg. At 19 weeks post-injection, the number of cells was about 14,636 ± 8,147 cells/leg. Although there was an increase in DTCs between weeks 1 and 5, it did not reach statistical significance (Fig. 7D, left panel). The level of DTCs detected between weeks 5 and 19 also did not reach statistical significance. However, there was a trend of continued increase in cell numbers over 19 weeks, suggesting that these DTCs were dormant or very slow-cycling in bone. These results are consistent with the studies by Lawson et al. (42), which showed that by intravital microscopy over 3 weeks some of the disseminated multiple myeloma cells were dormant/slow-cycling while others continued to proliferate in the bone marrow.

We further used intracardiac injection to examine the effect of disrupting p38MAPK signaling on tumor dormancy in bone. Disrupting p38MAPK signaling by expression of p38DN in C4-2B4 cells led to a significant 3-fold increase in the number of DTCs to about 43,859 ± 9,815 cells/leg at 19 weeks post-intracardiac injection (Fig. 7D, right panel). These observations are consistent with the involvement of p38MAPK in dormancy signaling.

Increases in tumor burden of C4-2B4-p38DN could be due to an increase in the proliferative activity or a decrease in dormant cells in the C4-2B4-p38DN tumor. We found that C4-2B4-p38DN cells showed a slightly higher proliferation rate (~30%) than C4-2B4-Vector control cells in vitro (Supplementary Fig. S4E), but there was no difference in the percent of quiescent cells between C4-2B4-p38DN and C4-2B4-Vector cells (Fig. 6C, blue bars). Thus, the increase in tumor burden of C4-2B4-p38DN is likely due to an increase in the

proliferative activity of C4-2B4-p38DN cells. Together, these results show that blocking p38MAPK activation via expression of dominant-negative p38MAPK overcame the effects of dormancy-inducing factors in the bone microenvironment and abrogated PCa tumor dormancy response in bone.

Lower TGFβRIII predicts poor clinical outcomes

Because dormancy induction requires the expression of TGFβRIII on PCa cells (Fig. 4B), PCa cells expressing lower TGFβRIII might be less able to enter into dormancy when disseminated to bone. If so, men with PCa that expressed lower TGFβRIII levels might have a shorter time between prostatectomy to the development of overt bone metastasis. Indeed, PCa patients with relatively lower levels of *TGFBR3* expression have shorter disease-specific survival in the Nakagawa dataset (13) (Fig. 7E). In addition, *TGFBR3* levels are significantly lower in the metastasis (n=19) than the primary (n=131) PCa tumor samples in the Taylor dataset (14) (Fig. 7F). Further, *TGFBR3* levels significantly correlate with PCa disease progression in the Lapointe dataset (15), in which primary PCa (n=59) expressed lower levels of *TGFBR3* than normal prostate tissue (n=39), and metastatic PCa (n=9) expressed the lowest levels of *TGFBR3* (Fig. 7F). These analyses support that lower levels of *TGFBR3* expression are associated with metastasis and poor clinical outcome of PCa.

Discussion

We examined how DTCs are initially induced into a dormant state in bone. Our findings elucidate that differentiated osteoblasts in the bone marrow are one cell type that regulates PCa tumor dormancy in bone. Our studies support a model in which differentiated osteoblasts secrete dormancy-inducing factors, including TGFβ2 and GDF10, which activate TGFβRIII signaling in PCa cells to stimulate p38MAPK phosphorylation and nuclear translocation. Nuclear p-p38 then phosphorylates the N-terminus of RB at pS249/pT252, leading to an increase in the CDK inhibitor p27 and blocking G1 cell cycle progression (Fig. 7G). Our studies provide a mechanistic pathway for the clinical observation that bone is the major site of PCa relapse. Understanding the mechanism underlying tumor dormancy provides the foundation for future development of strategies to prevent dormant tumors from emerging as overt bone metastasis.

Our studies identified factors secreted by differentiated osteoblasts that can regulate prostate tumor cell quiescence. GDF10 was first cloned from rat calvarial osteoblasts (42), and plays a role in osteoblast differentiation (43,44). We elucidate for the first time that osteoblast-derived GDF10 induces dormancy of PCa cells. Further, the levels of GDF10 and TGFβ2 are higher in differentiated compared to undifferentiated osteoblasts, indicating that the status of osteoblast differentiation may affect tumor dormancy. Studies by Lawson et al. (45) also showed that osteoblasts or bone-lining cells on quiescent bone surface were the major cell type in the bone marrow that provided dormancy factors to myeloma cells. Thus, it is likely that GDF10 and TGFβ2 are secreted from the bone-lining cells.

Additional factors in the bone microenvironment are also likely involved in PCa dormancy. In our osteoblast array analysis, we found GAS6, a factor reported to induce dormancy of PCa cells (24,46,47). We also found BMP family proteins including BMP5 and BMP3, but

not BMP4 or BMP7, in the microarray analysis (Fig. 2A). BMP7 was reported to be secreted by bone marrow stromal cells and was shown to induce dormancy of PC3 cells (17). Consistently, we did not detect BMP7 in either Day 0 or Day 30 osteoblasts (Fig. 2A). Thrombospondin-1 secreted by endothelial cells was also shown to sustain tumor cell quiescence (18). These observations suggest that many factors in the bone microenvironment affect dormancy.

We observed fluctuations of tumor growth in bone in our intrabone injection studies (Fig. 7A, Supplementary Figs. S4A–S4C). Lawson et al. (45) reported that they observed myeloma cells entering dormancy (dormancy switched on) when cells are located close to osteoblasts, but resumed proliferation (dormancy switched off) when cells are located farther away from osteoblasts in bone. This “on-and-off dormancy switch” has caused fluctuations in the dormancy status of myeloma cells. It is possible that a similar phenomenon might also occur in PCa cell dormancy in bone. When DTCs disseminate to bone, DTCs first encounter the trabeculae, which is enriched with osteoblasts. It is likely that osteoblast-secreted factors control the rate of cell proliferation and induce dormancy of the tumor cells near to the bone surface. The changes in the position of DTCs relative to bone over time may be one mechanism for DTCs to be reactivated after initial dormancy. Proliferating DTCs may also be regulated by cell death and survival pathways in the bone microenvironment. Our previous studies showed that the bone microenvironment also provides survival signals to PCa tumors, leading to therapy resistance (10). Thus, fluctuations of PCa tumor growth in bone may be due to both dormancy signals and survival signals provided by the bone microenvironment. Such dynamic interactions between tumor and the bone may regulate the temporal development of bone metastasis.

We found that activation of p38MAPK contributes to TGFβ2- and GDF10-mediated PCa cellular quiescence in vitro (Fig. 4 and 6) and PCa tumor dormancy in vivo (Fig. 7). Similarly, Adam et al. (48) and Chery et al. (49) showed that p38MAPK pathway activation may direct tumor cells to transit into a dormant state. Interestingly, Gubern et al. (8) demonstrated that p38MAPK phosphorylates the N-terminus of RB at S249/T252, which prevents its inactivation by cyclin-dependent kinases and results in inhibition of proliferation of cancer cells. Our studies showed that phospho-p38MAPK co-localizes with pS249/pT252-RB (Fig. 5), suggesting that RB is one of the substrates of p38MAPK activated by TGFβ2 or GDF10 treatment. RB upregulates p27, a cell cycle inhibitor and marker of quiescence, through p27 stabilization (50). Indeed, we found that dormant PCa cells express p27, suggesting that TGFβ2 or GDF10 treatment inhibits cell cycle progression at G1. Thus, our studies elucidate a p38MAPK-pS249/pT252-RB-p27 pathway as one mechanism by which PCa DTCs enter dormancy in bone (Fig. 7G).

PCa cells may exhibit different dormant phenotypes when disseminated to bone. Because paracrine factors signal through receptors, variations in receptor expression or the presence of tumor suppressor proteins such as RB in PCa cells due to tumor heterogeneity may lead to differences in the extent of dormancy response in the same tumor microenvironment. Indeed, we found that levels of TGFβRIII in PCa cells to be correlated with metastatic progression and poor clinical outcome of PCa. Additionally, the number of differentiated osteoblasts may affect the levels of dormancy-inducing factors. Furthermore, host immunity

may have a significant impact on cancer dormancy. Studies by Wu et al. (3) showed that when C4-2 cells were injected intracardially, only 1/5 athymic mice developed bone metastasis, whereas in SCID/bg mice that are more immune-impaired than the athymic nude mice, 3/7 and 2/7 developed lymph node and bone metastasis, respectively. In light of these studies, it is possible that the levels of bone-derived dormancy-inducing factors may be regulated by host immunity in different mouse strains. Together, these different variables may contribute in part to the difference in the time-to-bone metastasis and the incidence of bone metastasis among patients with advanced PCa (1).

We found that only a subset of available PCa cell lines became dormant in in vitro or in vivo studies. In our in vitro studies, we observed that C4-2B4, C4-2b, and PC3-mm2 but not 22Rv1 or BPH-1 cells showed dormancy response to TGFβ2 and GDF10 (Fig. 3D). We examined the expression of two molecules, i.e., TGFβRIII and RB, along the TGFβRIII-p38MAPK-pS249/pT252-RB-p27 pathway. Interestingly, we found that these PCa cell lines all express TGFβRIII and RB (Supplementary Fig. S5), suggesting that the differences in dormancy response in these PCa cells may lie elsewhere along the TGFβRIII-p38MAPK-pS249/pT252-RB-p27 pathway, for example, phosphorylation and nuclear translocation of p38MAPK, identified in our study. Some of the PCa cell lines may have intrinsic mechanisms that mediate reactivation from dormancy. We found that PC3-mm2 responded to TGFβ2 and GDF10 for dormancy induction (Fig. 3D), but they do not become dormant when injected into mouse femur. Thus, PC3-mm2 cells may have as-yet-unknown dormancy exit mechanisms that antagonize dormancy-inducing factors in the bone microenvironment. We have previously shown that PC3-mm2 cells express constitutively activated integrin β1 (10), which may lead to transition from quiescence to proliferation (19). Further, PC3-mm2 cells induce osteolytic bone lesions that may alter the bone microenvironment favoring PCa growth in bone. In breast cancer cells, VCAM1 expression was shown to lead to dormancy exit (51) and expression of Coco, a secreted BMP inhibitor, in MDA-MB-231 cells rendered these cells non-dormant (52). Our studies suggest that entry into and exit out of cellular dormancy may involve distinct pathways.

The identification of dormancy-inducing factors and their signaling mechanisms that lead to DTC quiescence suggests possibilities of developing strategies to prevent dormant tumors from emergence as overt bone metastasis. These could include strategies that either enhance or prevent loss of dormancy-inducing factor production. Further studies on the molecular mechanisms regulating entry into and exit out of dormancy may reveal specific targets for therapeutic manipulation.

Supplementary Material

Refer to Web version on PubMed Central for supplementary material.

Acknowledgments

This work was supported by grants from the NIH R01CA174798 to S.-H. Lin, NIH 5P50CA140388 to C. Logothetis and S.-H. Lin, NIH P30CA16672 Core grant to M.D. Anderson Cancer Center (PI: R. DePinho); Cancer Prevention Research Institute of Texas CPRIT RP150179 to S.-H. Lin and L.-Y. Yu-Lee, CPRIT RP150282 to G.E. Gallick and S.-H. Lin; and Sister Institute Network Fund at U. Texas M.D. Anderson Cancer Center to S.-H. Lin.

References

1. Ahove DA, Hoffman KE, Hu JC, Choueiri TK, D'Amico AV, Nguyen PL. Which patients with undetectable PSA levels 5 years after radical prostatectomy are still at risk of recurrence?--implications for a risk-adapted follow-up strategy. Urology. 2010; 76(5):1201–5. [PubMed: 20709376]
2. Logothetis C, Lin S-H. Osteoblasts in prostate cancer metastasis to bone. Nature Reviews Cancer. 2005; 5:21–28. [PubMed: 15630412]
3. Wu TT, Sikes RA, Cui Q, Thalmann GN, Kao C, Murphy CF, et al. Establishing human prostate cancer cell xenografts in bone: induction of osteoblastic reaction by prostate-specific antigen-producing tumors in athymic and SCID/bg mice using LNCaP and lineage-derived metastatic sublines. Int J Cancer. 1998; 77:887–94. [PubMed: 9714059]
4. Thalmann GN, Sikes RA, Wu TT, Degeorges A, Chang SM, Ozen M, et al. LNCaP progression model of human prostate cancer: androgen-independence and osseous metastasis. Prostate. 2000; 44:91–103. [PubMed: 10881018]
5. Thalmann GN, Anezinis PE, Chang S, Zhau HE, Kim E, Hopwood VL, et al. Androgen-independent cancer progression and bone metastasis in the LNCaP model of human prostate cancer. Cancer Res. 1994; 54:2577–81. [PubMed: 8168083]
6. Wainstein MA, He F, Robinson D, Kung HJ, Schwartz S, Giaconia JM, et al. CWR22: androgen-dependent xenograft model derived from a primary human prostatic carcinoma. Cancer Res. 1994; 54(23):6049–52. [PubMed: 7525052]
7. Sramkoski RM, Pretlow TG 2nd, Giaconia JM, Pretlow TP, Schwartz S, Sy MS, et al. A new human prostate carcinoma cell line, 22Rv1. In Vitro Cell Dev Biol Anim. 1999; 35(7):403–9. [PubMed: 10462204]
8. Gubern A, Joaquin M, Marques M, Maseres P, Garcia-Garcia J, Amat R, et al. The N-Terminal Phosphorylation of RB by p38 Bypasses Its Inactivation by CDKs and Prevents Proliferation in Cancer Cells. Mol Cell. 2016; 64(1):25–36. [PubMed: 27642049]
9. Lin SH, Cheng CJ, Lee YC, Ye X, Tsai WW, Kim J, et al. A 45-kDa ErbB3 secreted by prostate cancer cells promotes bone formation. Oncogene. 2008; 27(39):5195–203. [PubMed: 18490922]
10. Lee YC, Jin JK, Cheng CJ, Huang CF, Song JH, Huang M, et al. Targeting constitutively activated beta1 integrins inhibits prostate cancer metastasis. Molecular cancer research: MCR. 2013; 11(4): 405–17. [PubMed: 23339185]
11. Chu K, Cheng CJ, Ye X, Lee YC, Zurita AJ, Chen DT, et al. Cadherin-11 promotes the metastasis of prostate cancer cells to bone. Molecular cancer research: MCR. 2008; 6(8):1259–67. [PubMed: 18708358]
12. Somwar R, Koterski S, Sweeney G, Sciotti R, Djuric S, Berg C, et al. A dominant-negative p38 MAPK mutant and novel selective inhibitors of p38 MAPK reduce insulin-stimulated glucose uptake in 3T3-L1 adipocytes without affecting GLUT4 translocation. J Biol Chem. 2002; 277(52): 50386–95. [PubMed: 12393894]
13. Nakagawa T, Kollmeyer TM, Morlan BW, Anderson SK, Bergstralh EJ, Davis BJ, et al. A tissue biomarker panel predicting systemic progression after PSA recurrence post-definitive prostate cancer therapy. PLoS One. 2008; 3(5):e2318. [PubMed: 18846227]
14. Taylor BS, Schultz N, Hieronymus H, Gopalan A, Xiao Y, Carver BS, et al. Integrative genomic profiling of human prostate cancer. Cancer Cell. 2010; 18(1):11–22. [PubMed: 20579941]
15. Lapointe J, Li C, Higgins JP, van de Rijn M, Bair E, Montgomery K, et al. Gene expression profiling identifies clinically relevant subtypes of prostate cancer. Proc Natl Acad Sci U S A. 2004; 101(3):811–6. [PubMed: 14711987]
16. Bragado P, Estrada Y, Parikh F, Krause S, Capobianco C, Farina HG, et al. TGF-beta2 dictates disseminated tumour cell fate in target organs through TGF-beta-RIII and p38alpha/beta signalling. Nat Cell Biol. 2013; 15(11):1351–61. [PubMed: 24161934]
17. Kobayashi A, Okuda H, Xing F, Pandey PR, Watabe M, Hirota S, et al. Bone morphogenetic protein 7 in dormancy and metastasis of prostate cancer stem-like cells in bone. J Exp Med. 2011; 208(13):2641–55. [PubMed: 22124112]

18. Ghajar CM, Peinado H, Mori H, Matei IR, Evason KJ, Brazier H, et al. The perivascular niche regulates breast tumour dormancy. Nat Cell Biol. 2013; 15(7):807–17. [PubMed: 23728425]
19. Barkan D, Kleinman H, Simmons JL, Asmussen H, Kamaraju AK, Hoenorhoff MJ, et al. Inhibition of metastatic outgrowth from single dormant tumor cells by targeting the cytoskeleton. Cancer Res. 2008; 68(15):6241–50. [PubMed: 18676848]
20. El Touny LH, Vieira A, Mendoza A, Khanna C, Hoenerhoff MJ, Green JE. Combined SFK/MEK inhibition prevents metastatic outgrowth of dormant tumor cells. J Clin Invest. 2014; 124(1):156–68. [PubMed: 24316974]
21. Poole KE, van Bezooijen RL, Loveridge N, Hamersma H, Papapoulos SE, Lowik CW, et al. Sclerostin is a delayed secreted product of osteocytes that inhibits bone formation. FASEB J. 2005; 19(13):1842–4. [PubMed: 16123173]
22. Salm SN, Burger PE, Coetzee S, Goto K, Moscatelli D, Wilson EL. TGF-{beta} maintains dormancy of prostatic stem cells in the proximal region of ducts. J Cell Biol. 2005; 170(1):81–90. [PubMed: 15983059]
23. Aguirre-Ghiso JA. Models, mechanisms and clinical evidence for cancer dormancy. Nat Rev Cancer. 2007; 7(11):834–46. [PubMed: 17957189]
24. Shiozawa Y, Pedersen EA, Patel LR, Ziegler AM, Havens AM, Jung Y, et al. GAS6/AXL axis regulates prostate cancer invasion, proliferation, and survival in the bone marrow niche. Neoplasia. 2010; 12(2):116–27. [PubMed: 20126470]
25. Delworth M, Nishioka K, Pettaway C, Gutman M, Killion J, Voneschenbach A, et al. Systemic administration of 4-amidinoindanon-1-(2′-amidino)-hydrazone, a new inhibitor of s-adenosylmethionine decarboxylase, produces cytostasis of human prostate-cancer in athymic nude-mice. Int J Oncol. 1995; 6(2):293–9. [PubMed: 21556536]
26. Hayward SW, Dahiya R, Cunha GR, Bartek J, Deshpande N, Narayan P. Establishment and characterization of an immortalized but non-transformed human prostate epithelial cell line: BPH-1. In Vitro Cell Dev Biol Anim. 1995; 31(1):14–24. [PubMed: 7535634]
27. Lopez-Casillas F, Wrana JL, Massague J. Betaglycan presents ligand to the TGF beta signaling receptor. Cell. 1993; 73(7):1435–44. [PubMed: 8391934]
28. Upadhyay G, Yin Y, Yuan H, Li X, Derynck R, Glazer RI. Stem cell antigen-1 enhances tumorigenicity by disruption of growth differentiation factor-10 (GDF10)-dependent TGF-beta signaling. Proc Natl Acad Sci U S A. 2011; 108(19):7820–5. [PubMed: 21518866]
29. Cheng CW, Hsiao JR, Fan CC, Lo YK, Tzen CY, Wu LW, et al. Loss of GDF10/BMP3b as a prognostic marker collaborates with TGFBR3 to enhance chemotherapy resistance and epithelial-mesenchymal transition in oral squamous cell carcinoma. Molecular carcinogenesis. 2016; 55(5): 499–513. [PubMed: 25728212]
30. Li S, Nie EH, Yin Y, Benowitz LI, Tung S, Vinters HV, et al. GDF10 is a signal for axonal sprouting and functional recovery after stroke. Nature neuroscience. 2015; 18(12):1737–45. [PubMed: 26502261]
31. Andres JL, Ronnstrand L, Cheifetz S, Massague J. Purification of the transforming growth factor-beta (TGF-beta) binding proteoglycan betaglycan. J Biol Chem. 1991; 266(34):23282–7. [PubMed: 1744125]
32. Aguirre-Ghiso JA, Liu D, Mignatti A, Kovalski K, Ossowski L. Urokinase receptor and fibronectin regulate the ERK(MAPK) to p38(MAPK) activity ratios that determine carcinoma cell proliferation or dormancy in vivo. Mol Biol Cell. 2001; 12(4):863–79. [PubMed: 11294892]
33. Aguirre-Ghiso JA, Estrada Y, Liu D, Ossowski L. ERK(MAPK) activity as a determinant of tumor growth and dormancy; regulation by p38(SAPK). Cancer Res. 2003; 63(7):1684–95. [PubMed: 12670923]
34. Ranganathan AC, Adam AP, Aguirre-Ghiso JA. Opposing roles of mitogenic and stress signaling pathways in the induction of cancer dormancy. Cell cycle. 2006; 5(16):1799–807. [PubMed: 16929185]
35. Massague J. TGFbeta in Cancer. Cell. 2008; 134(2):215–30. [PubMed: 18662538]
36. Moustakas A, Heldin CH. The regulation of TGFbeta signal transduction. Development. 2009; 136(22):3699–714. [PubMed: 19855013]

37. Yamashita M, Fatyol K, Jin C, Wang X, Liu Z, Zhang YE. TRAF6 mediates Smad-independent activation of JNK and p38 by TGF-beta. Mol Cell. 2008; 31(6):918–24. [PubMed: 18922473]
38. Parvani JG, Taylor MA, Schiemann WP. Noncanonical TGF-beta signaling during mammary tumorigenesis. Journal of mammary gland biology and neoplasia. 2011; 16(2):127–46. [PubMed: 21448580]
39. Satcher RL, Pan T, Bilen MA, Li X, Lee YC, Ortiz A, et al. Cadherin-11 endocytosis through binding to clathrin promotes cadherin-11-mediated migration in prostate cancer cells. J Cell Sci. 2015; 128(24):4629–41. [PubMed: 26519476]
40. Soderberg O, Gullberg M, Jarvius M, Ridderstrale K, Leuchowius KJ, Jarvius J, et al. Direct observation of individual endogenous protein complexes in situ by proximity ligation. Nat Methods. 2006; 3(12):995–1000. [PubMed: 17072308]
41. Fidler IJ. The pathogenesis of cancer metastasis: the 'seed and soil' hypothesis revisited. Nat Rev Cancer. 2003; 3:453–8. [PubMed: 12778135]
42. Takao M, Hino J, Takeshita N, Konno Y, Nishizawa T, Matsuo H, et al. Identification of rat bone morphogenetic protein-3b (BMP-3b), a new member of BMP-3. Biochemical and biophysical research communications. 1996; 219(2):656–62. [PubMed: 8605043]
43. Hino J, Matsuo H, Kangawa K. Bone morphogenetic protein-3b (BMP-3b) gene expression is correlated with differentiation in rat calvarial osteoblasts. Biochemical and biophysical research communications. 1999; 256(2):419–24. [PubMed: 10079200]
44. Kaihara S, Bessho K, Okubo Y, Sonobe J, Komatsu Y, Miura M, et al. Over expression of bone morphogenetic protein-3b (BMP-3b) using an adenoviral vector promote the osteoblastic differentiation in C2C12 cells and augment the bone formation induced by bone morphogenetic protein-2 (BMP-2) in rats. Life sciences. 2003; 72(15):1683–93. [PubMed: 12559390]
45. Lawson MA, McDonald MM, Kovacic N, Hua Khoo W, Terry RL, Down J, et al. Osteoclasts control reactivation of dormant myeloma cells by remodelling the endosteal niche. Nat Commun. 2015; 6:8983. [PubMed: 26632274]
46. Taichman RS, Patel LR, Bedenis R, Wang J, Weidner S, Schumann T, et al. GAS6 receptor status is associated with dormancy and bone metastatic tumor formation. PLoS One. 2013; 8(4):e61873. [PubMed: 23637920]
47. Yumoto K, Eber MR, Wang J, Cackowski FC, Decker AM, Lee E, et al. Axl is required for TGF-beta2-induced dormancy of prostate cancer cells in the bone marrow. Scientific reports. 2016; 6:36520. [PubMed: 27819283]
48. Adam AP, George A, Schewe D, Bragado P, Iglesias BV, Ranganathan AC, et al. Computational identification of a p38SAPK-regulated transcription factor network required for tumor cell quiescence. Cancer Res. 2009; 69(14):5664–72. [PubMed: 19584293]
49. Chery L, Lam HM, Coleman I, Lakely B, Coleman R, Larson S, et al. Characterization of single disseminated prostate cancer cells reveals tumor cell heterogeneity and identifies dormancy associated pathways. Oncotarget. 2014; 5(20):9939–51. [PubMed: 25301725]
50. Dick FA, Rubin SM. Molecular mechanisms underlying RB protein function. Nat Rev Mol Cell Biol. 2013; 14(5):297–306. [PubMed: 23594950]
51. Lu X, Mu E, Wei Y, Riethdorf S, Yang Q, Yuan M, et al. VCAM-1 promotes osteolytic expansion of indolent bone micrometastasis of breast cancer by engaging alpha4beta1-positive osteoclast progenitors. Cancer Cell. 2011; 20(6):701–14. [PubMed: 22137794]
52. Gao H, Chakraborty G, Lee-Lim AP, Mo Q, Decker M, Vonica A, et al. The BMP inhibitor Coco reactivates breast cancer cells at lung metastatic sites. Cell. 2012; 150(4):764–79. [PubMed: 22901808]

Statement of Significance

Findings provide mechanistic insights into the dormancy of metastatic prostate cancer in the bone and offer a rationale for developing strategies to prevent prostate cancer recurrence in the bone.

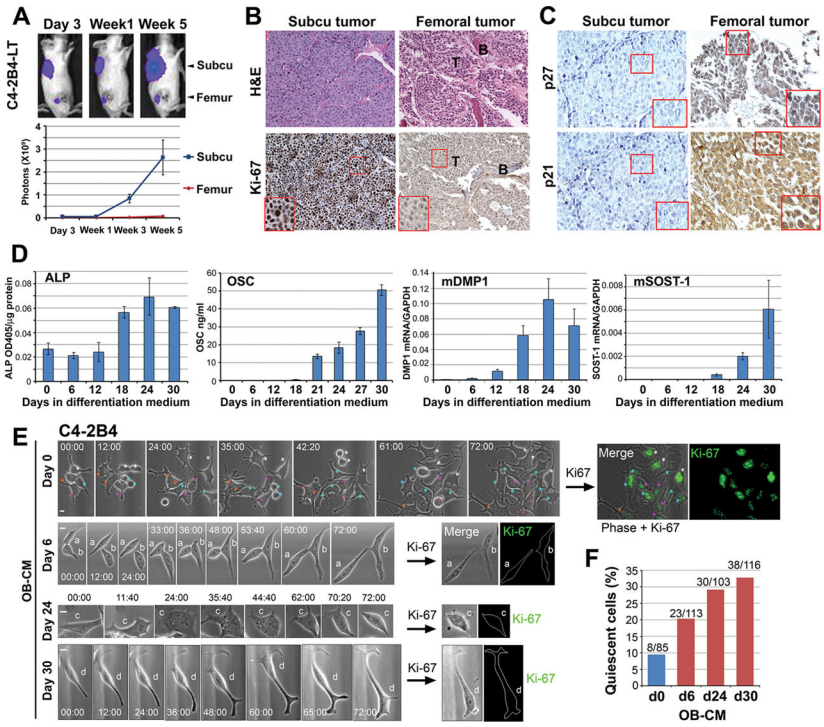

Figure 1. Osteoblasts in bone microenvironment confer dormancy on C4-2B4 tumor

(A) C4-2B4-LT cells (1×10^6) were injected subcutaneously (subcu) (n=10) or into the femur of SCID mice (n=10). Tumor growth was monitored by bioluminescence. Consecutive tissue sections were stained as follows: **(B)** H&E or immunostained with anti-Ki-67 (200X); (**C**) anti-p27 or anti-p21 (400 X). Box, enlarged. T, tumor; B, bone. **(D)** PMOs during differentiation in culture. Cell lysates were used for alkaline phosphatase activity, conditioned media for osteocalcin ELISA, and RNAs for qRT-PCR of mDMP1 and mSOST-1. **(E)** Live-cell imaging (h:min) of C4-2B4 cells treated for 72 h with Day 0, 6, 24 and 30 osteoblast-conditioned medium (OB-CM). Colored asterisks, Day 0 progenies. Round cells are mitotic. Cells a-d, quiescent C4-2B4 cells in Day 6, 24 or 30 OB-CM. Following time-lapse, cells were immunostained for Ki-67. Cell outlines are traced. All bars, 10 μm. **(F)** Quantification of OB-CM-treated quiescent C4-2B4 cells that did not divide over 55–72 h relative to total cells examined. Representative of two independent experiments.

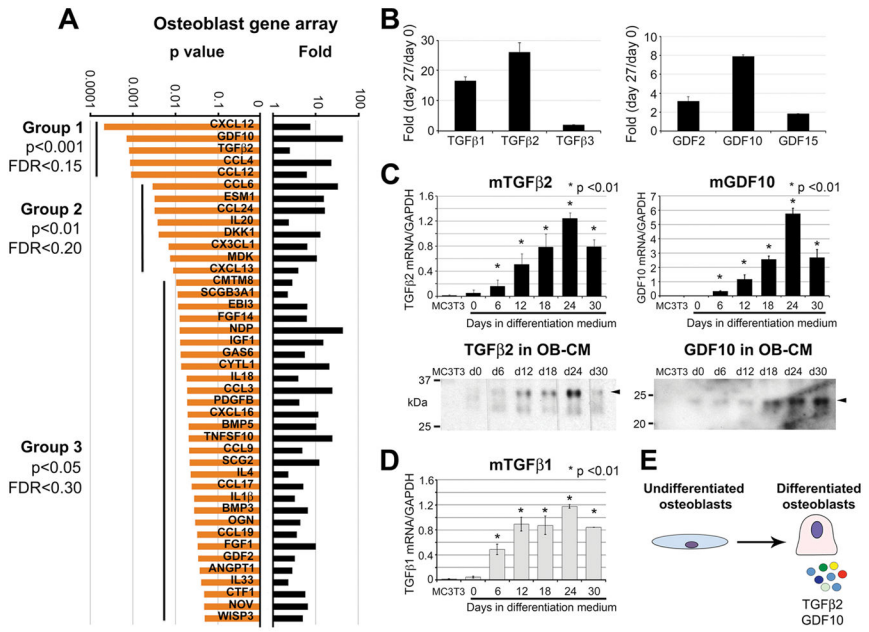

Figure 2. Gene array analyses of osteoblasts before and after culturing in differentiation medium for 30 days

(A) RNAs from undifferentiated (Day 0) or differentiated (Day 30) osteoblasts were used in a whole-genome microarray analysis. 42 transcripts encoding secreted factors upregulated in Day 30 osteoblasts were subdivided into three groups, based on p values and false discovery rate (FDR). Fold increase is shown on right. **(B)** RNA levels of select TGFβ and GDF family genes during osteoblast differentiation. **(C)** TGFβ2 or GDF10 expression by qRT-PCR (upper) or western blot (lower). Undifferentiated osteoblast precursor MC3T3-E1 cells were used as a control. **(D)** TGFβ1 RNA levels. *p < 0.01 by *t* test. **(E)** TGFβ2 and GDF10 are two of many factors upregulated and secreted by osteoblasts over 30 days of differentiation in culture.

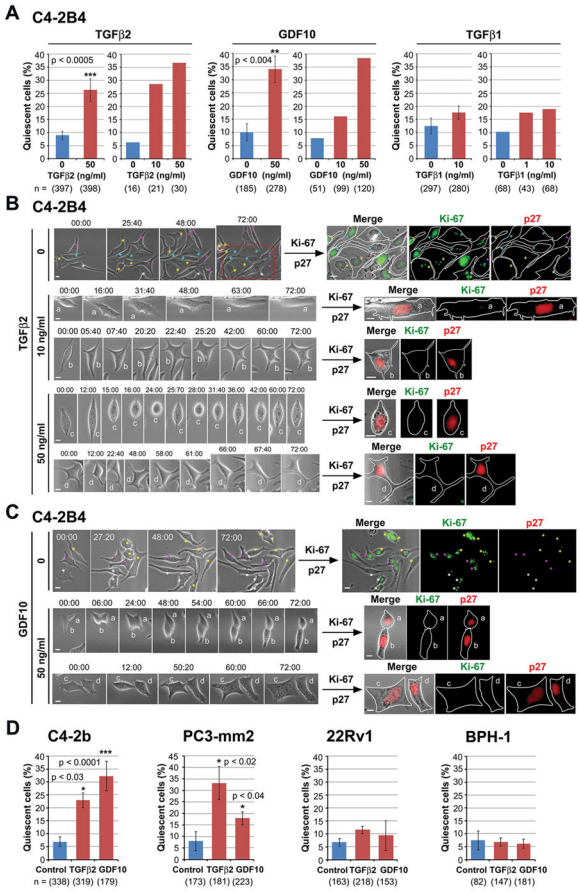

Figure 3. TGFβ2 and GDF10 induce PCa cellular quiescence in vitro

(A) C4-2B4 cells treated with TGFβ2, GDF10 or TGFβ1 for 72 h were analyzed by live-cell imaging. Quiescent cells that did not divide in 60–72 h relative to total cells counted were quantified (mean ± s.e.m). n cells were analyzed in multiple experiments: TGFβ2 (N=5–8), GDF10 (N=4), and TGFβ1 (N=5), except for TGFβ2 or GDF10 dose response (N=1). P values were by *t* test. Live-cell images (h:min) of cells treated with TGFβ2 **(B)** or GDF10 **(C)**, followed by co-immunostaining for Ki-67 and p27. Colored asterisks, control cell progenies. Red box, enlarged. Cells a-d, quiescent cells following TGFβ2 or GDF10 treatment. All bars, 10 μm. **(D)** Cellular quiescence of several other PCa cells treated and analyzed as in (A) in multiple experiments: C4-2b (N=3–5), PC3-mm2 (N=2–3), 22Rv1 (N=2–3), BPH-1 (N=2–3).

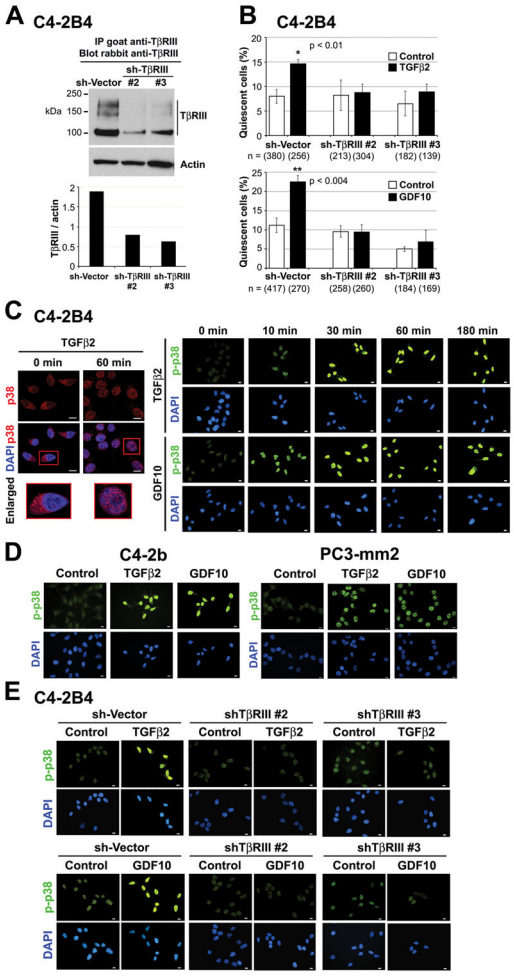

Figure 4. TGFβRIII receptor and activation of p38MAPK signaling mediate TGFβ2 and GDF10 dormancy-inducing effects in PCa cells

(A) TGFβRIII levels in knockdown clones C4-2B4-shTβRIII-#2 and #3 were analyzed by immunoprecipitation followed by immunoblotting, quantified against pGIPZ-sh-Vector cells, and signals normalized against actin controls. Bar, TGFβRIII 100-kDa core protein and glycosylated forms. **(B)** Cells in (A) were treated with 50 ng/ml TGFβ2 or GDF10 for 72 h. Cellular quiescence was determined by live-cell imaging. n cells were monitored in N=3–5 experiments, except for shTβRIII-#3 cells (N=2). P values are by *t* test. **(C)** Left, C4-2B4 cells were treated with TGFβ2, immunostained for p38MAPK, and counterstained with DAPI. Images were captured by confocal microscopy. Box, enlarged. Right, phospho-p38MAPK (p-p38) immunostaining following TGFβ2 or GDF10 time course. **(D)** C4-2b and PC3-mm2 cells and **(E)** C4-2B4-sh-Vector, C4-2B4-shTβRIII-#2 and C4-2B4-shTβRIII-#3 cells were immunostained for p-p38 after treatment with TGFβ2 or GDF10 for 60 min. All bars, 10 μm.

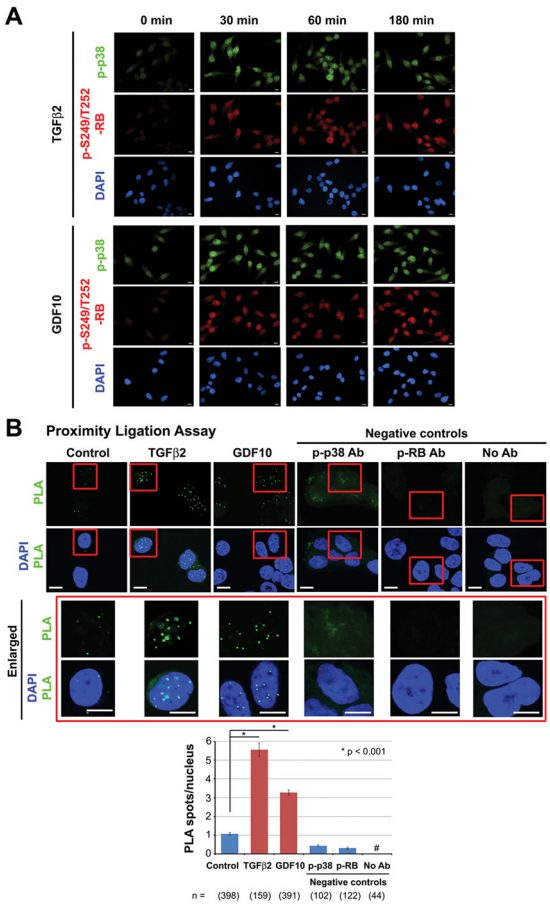

Figure 5. Phospho-p38MAPK and novel N-terminal phospho-S249/T252-RB colocalize in the nucleus of TGFβ2- or GDF10-treated C4-2B4 cells

(A) C4-2B4 cells were treated with 50 ng/ml TGFβ2 or GDF10 and co-immunostained for p-p38 and phospho-S249/T252-RB (8). **(B)** Cells treated as in (A) for 180 min were co-immunostained as in (A), followed with proximity ligation assay. Cells incubated with either primary antibodies alone or no antibodies served as negative controls. Boxes, enlarged. All bars, 10 μm. PLA spots/nucleus were quantified in n nuclei. P values are by *t* test. #, no spots detected.

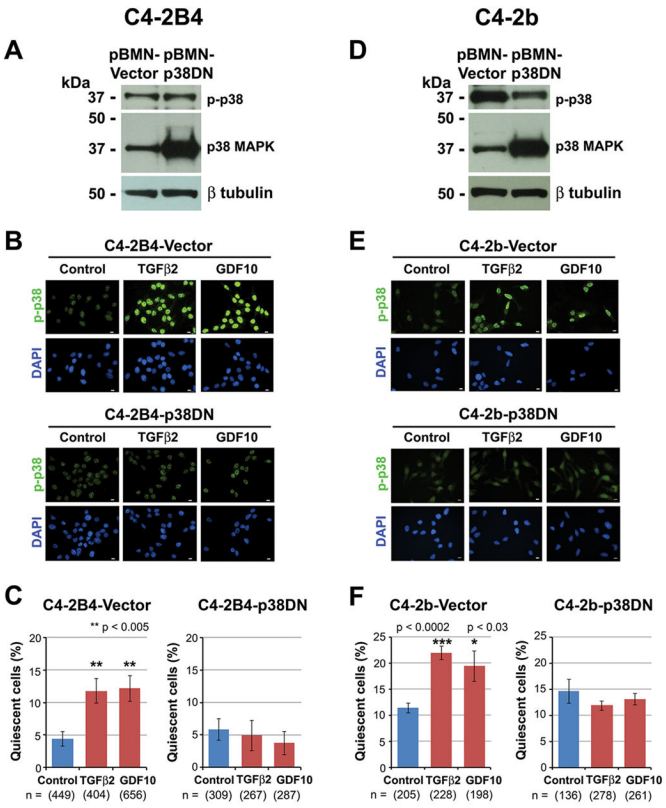

Figure 6. Dominant-negative p38MAPK prevents dormancy induction by TGFβ2 or GDF10 in PCa cells in vitro

(A) C4-2B4 cells stably-expressing empty vector or p38DN were examined by western blot for p-p38 followed by p38MAPK. β-tubulin, loading control. **(B)** Cells in (A) were treated with 50 ng/ml TGFβ2 or GDF10 for 60 min and immunostained for p-p38. **(C)** Cells in (A) were treated with TGFβ2 or GDF10 for 72 h. Cellular quiescence was determined by live-cell imaging. n cells were monitored in multiple experiments: C4-2B4-Vector (N=5–7), C4-2B4-p38DN (N=4–5). P values are by *t* test. **(D)** C4-2b-Vector or C4-2b-p38DN cells were generated and examined by western blot as in (A). **(E)** Cells in (D) were treated as in (B) and immunostained for p-p38. All bars, 10 μm. **(F)** Cellular quiescence in C4-2b-Vector or C4-2b-p38DN cells after TGFβ2 or GDF10 incubation was determined as in (C). n cells were followed in multiple experiments: C4-2b-Vector (N=4–5), C4-2b-p38DN (N=3–5).

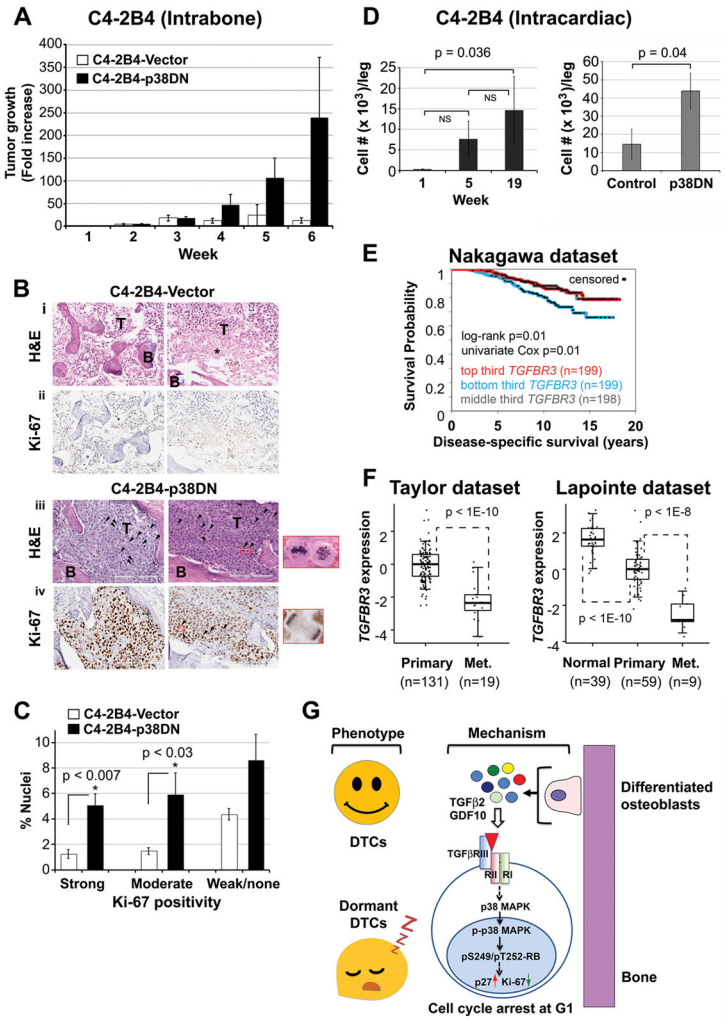

Figure 7. Dominant-negative p38MAPK prevents dormancy in vivo and lower TGFβRIII expression is associated with poor survival rates in human PCa

(A) Intrabone injection. C4-2B4-Vector or C4-2B4-p38DN cells (1 x 10^6) were injected into the femur of SCID mice (n=5 each). Tumor growth was monitored by bioluminescence and expressed as fold increase relative to Week 1. **(B)** Consecutive sections of C4-2B4-Vector (i, ii)- or C4-2B4-p38DN (iii, iv)-derived femoral tumors in (A) were analyzed by H&E and Ki-67. Boxes, enlarged mitotic cells: (iii), metaphase (left), prometaphase (right); (iv), cells separating in telophase. T, tumor; B, bone; *, dead cells; arrowheads, mitotic cells. 200X. **(C)** Quantification of Ki-67 levels in nuclei of C4-2B4 tumors using the Aperio ImageScope software. **(D)** Intracardiac injection. Left panel, C4-2B4 cells (1 × 10^6) were injected into the left ventricle of SCID mice. At the indicated times, total femur and tibia DNA was harvested from hind legs and subjected to quantitative PCR for human *Alu* repetitive sequence, using 20 ng DNA. DNA from C4-2B4 was used to generate a standard curve for calculating cell numbers/20 ng DNA. The total cell numbers/leg was then calculated based on total DNA per mouse leg. Right panel, C4-2B4-Vector cells or C4-2B4-p38DN cells (1 x 10^6) were injected into the left ventricle of SCID mice (n=3 each). At 19 weeks post-injection, *Alu* PCR was performed. P values are by *t* test. NS, not significant. **(E)** Kaplan-Meier plots for correlations

of *TGFBR3* expression with disease-specific survival of PCa patients (Nakagawa dataset) (13). Groups with highest ("top third"), lowest ("bottom third"), and intermediate ("middle third") *TGFBR3* mRNA levels were compared. P values are determined by univariate Cox and stratified log-rank test. n, number of patients. **(F)** Box plots show correlations of *TGFBR3* expression with PCa metastatic potential (Taylor dataset) (14) and PCa metastatic progression (Lapointe dataset) (15). P values are by *t* test. **(G)** Model for PCa tumor dormancy in bone. See text.